Title

Photoelectrochemical CO2 Reduction toward Multicarbon Products with Silicon Nanowire Photocathodes Interfaced with Copper Nanoparticles

Journal

Journal of the American Chemical Society, 144(18)

ISSN

0002-7863

Authors

Roh, Inwhan
Yu, Sunmoon
Lin, Chung-Kuan
et al.

Publication Date

2022-05-11

DOI

10.1021/jacs.2c03702

Peer reviewed

Photoelectrochemical CO_2 reduction towards multi-carbon products with silicon nanowire photocathodes interfaced with copper nanoparticles

Inwhan Roh[†,‡], Sunmoon Yu[§,||], Chung-Kuan Lin[†], Sheena Louisia[†,||], Stefano Cestellos-Blanco[§], Peidong Yang[†,‡,§,||,#*]

[†]Department of Chemistry, University of California, Berkeley, California 94720, United States
[‡]Liquid Sunlight Alliance, Lawrence Berkeley National Laboratory, Berkeley, California, 94720, United States
[§]Department of Materials Science and Engineering, University of California, Berkeley, California 94720, United States
[||]Chemical Sciences Division, Lawrence Berkeley National Laboratory, Berkeley, California 94720, United States
[#]Kavli Energy NanoScience Institute, Berkeley, California 94720, United States
*p_yang@berkeley.edu

Supporting Information Placeholder

ABSTRACT: The development of photoelectrochemical systems for converting CO_2 into chemical feedstocks offers an attractive strategy for clean energy storage by directly utilizing solar energy, but selectivity and stability for these systems has thus been limited. Here, we interface silicon nanowire (SiNW) photocathodes with a copper nanoparticle (CuNP) ensemble to drive efficient photoelectrochemical CO_2 conversion to multi-carbon products. This integrated system enables CO_2-to-C_2H_4 conversion with faradaic efficiency approaching 25% and partial current densities above 2.5 mA/cm^2 at -0.50 V vs RHE while the nanowire photocathodes deliver 350 mV of photovoltage under 1 sun illumination. Under 50 hours of continual bias and illumination, CuNP/SiNW can sustain stable photoelectrochemical CO_2 reduction. These results demonstrate the nanowire/catalyst system as a powerful modular platform to achieve stable photoelectrochemical CO_2 reduction and the feasibility to facilitate complex reactions towards multi-carbons using generated photocarriers.

The effects of CO_2 emissions on global warming creates a pressing need for clean alternative fuels for energy storage and transport that overcome the intermittent nature of certain types of renewable energy (solar, hydro, and wind).[1-4] One such tactic is artificial photosynthesis in which solar energy is stored in the form of chemical bonds by using photogenerated charges to drive uphill reactions.[5] This can be achieved by combining semiconductors, to harvest light, with inorganic or biological cocatalysts capable of driving chemical reactions with the generated charge carriers.[6,7] While most initial efforts using inorganic electrocatalysts were directed toward water splitting,[8] there have been recent reports showing photoelectrochemical (PEC) CO_2 reduction (CO_2R) towards single-carbon products such as carbon monoxide, formate, and methane.[9-11] However, despite the development of inorganic electrocatalysts for stable and selective multi-carbon formation demonstrated in the electrochemical CO_2R community,[12] literature remains sparse in seeing similar advancements for PEC CO_2R.

Designing a photoelectrode requires consideration of its light absorption properties and cocatalyst integration without parasitic light absorption.[13] In this aim, SiNW arrays can be utilized which offer a large surface area, a conduction band level of -0.5 V vs SHE, favorable light trapping properties, and orthogonalization of light absorption and charge separation for efficient carrier charge extraction.[14-17] In addition, a radial n^+p junction can be formed to increase the photovoltage by 250 mV[18] and to drive photogenerated holes away from the surface to prevent photocorrosion.[19] This array has been used to demonstrate a fully integrated water splitting photoelectrode using a single optical path device geometry,[20] a microorganism/semiconductor interface for unassisted solar CO_2R into acetate at near unit selectivity,[4,21] and a directed assembly of colloidal nanoparticles for CO_2R into CO at 80% faradaic efficiency (FE).[22]

The large surface area of the NW array is especially important for CO_2R because it allows a large mass loading of catalyst. High selectivity towards multi-carbon products can be achieved by controlling the current density at a given potential by modulating the surface area of copper,[23] the only known metal capable of carbon-carbon coupling,[24] and by using nanostructures with undercoordinated sites.[25] This was attributed to having to build up a necessary concentration of intermediates (carbon monoxide) in its microenvironment for carbon-carbon coupling.[26] Systems using planar silicon for wet-side illumination CO_2R (incident light, catalyst, and electrolyte on same side) show low current densities and selectivity toward multi-carbons due to low mass loading[27,28] while a microwire array with large mass loading (>300 μg/cm^2) showed limited stability (≤1 hour) likely due to catalyst deactivation.[29] Considering that practical applications require long term operations with high current densities (mA scale),[30] it remains a major challenge to discover more durable and selective PEC CO_2R systems.

In this work, we demonstrate stable aqueous PEC CO_2R by interfacing CuNPs to n^+p-SiNW photocathodes. This catalytic system yields high C_2H_4 FE (~25%) and appreciable partial current densities (>2.5 mA/cm^2) at -0.50 V vs RHE, a reduction

of applied potential by about ~350 mV from its electrochemical counterpart. The CuNPs structurally evolve under bias, exposing the silicon surface and allowing tolerance to higher mass loadings without adverse light blocking. This system also maintains stable CO_2R of over 50 hours under continuous bias and illumination which show the benefits of combining highly active and stable CuNPs with the benefits of the SiNW array.

7 nm CuNPs were assembled onto SiNWs by using a previously reported drop-cast directed assembly process (Figure 1).[22] Scanning electron microscopy (SEM) images (Figure 1d) confirm that drop-casting coats CuNPs uniformly along the NW with 20 μg/cm² mass loading achieving almost a monolayer coverage of the surface (Figure S1). This NW array has a calculated surface area of 7.6 cm² with a theoretical mass loading of 25.7 μg/cm² of CuNPs for complete monolayer coverage (see Methods). The SEM observation is in good agreement with the theoretical value which suggests that the nanoparticles (NPs) disperse well across the substrate.

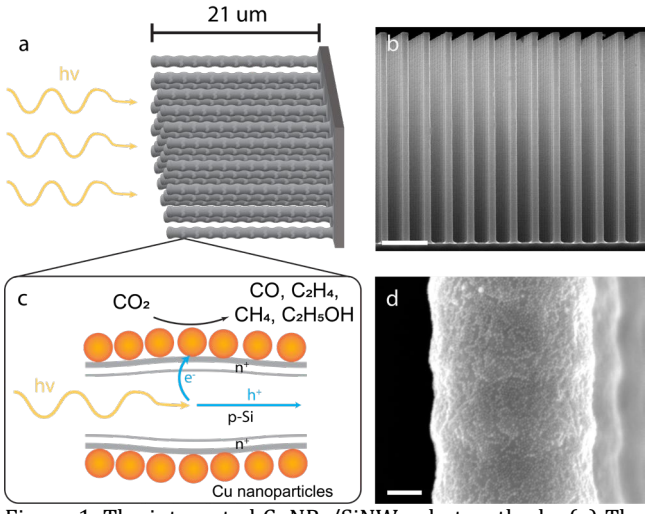

Figure 1. The integrated CuNPs/SiNWs photocathode. (a) The arrays have nanowire diameters of 400 nm, length of 21 μm, and pitch of 2 μm. (b) The SEM image (scale bar 4 μm) of the NW array. (c) Schematic illustration showing the dopant layer and charge separation and (d) the corresponding SEM image (scale bar 100 nm).

The PEC performance of this CuNP/SiNW array was tested under 100 mW/cm² of air mass (AM) 1.5 simulated sunlight in CO_2-saturated 0.1 M $KHCO_3$ (Figure 2a). The generated current under illumination principally results from photogenerated electrons (Figure S2) and the photovoltage produced by SiNWs shifts the CO_2R onset potential positively by 350 mV with the photocurrent reaching >10 mA/cm² at -0.50 V vs RHE (Figure S3). Using Ar-purged 0.1 M $KHCO_3$ show no hydrocarbon products and $^{13}CO_2$ isotope labeling shows that CO_2R products are formed from the input CO_2 gas (Figures S4, S5).

However, the overall photocurrent alone is not a beneficial metric as there many competing reactions during CO_2R including the hydrogen evolution reaction (HER).[31] Figure 2b shows the selectivity for CO_2R gas products at different mass loadings. These CuNPs are known to structurally evolve *in situ* or "electrochemically scramble" to form an undercoordinated active state that features high turnover rates for multi-carbon formation at seven times that of polycrystalline or oxide-derived copper catalysts.[25] This evolution and thus performance is dependent on the initial packing of the nanoparticles where low densities favored $2e^-$ products and higher densities favored $>2e^-$ products. We find that the optimal loading density is 1-2 monolayers of CuNPs (40 μg/cm²) which is consistent with previous reports.[32]

The activity towards C_2H_4 for CuNP/SiNW is shown in Figure 2c,d. At -0.45 V vs RHE, FE_{C2H4} reaches over 20% as the main product of CO_2R and achieves 25 ± 6% at -0.55 V vs RHE (Figure 2c) which is the highest reported value for wet-side illumination PEC CO_2R (Table S1). With 40 μg/cm² of CuNPs, j_{C2H4} reaches 2.5 mA/cm² whereas over sevenfold mass loading was necessary in a similar system using photoelectrodeposited copper to reach a comparable partial current density, but at a lower FE_{C2H4}.[29] This highlights the importance of using highly active catalysts that are uniformly deposited to effectively utilize the generated charge carriers.

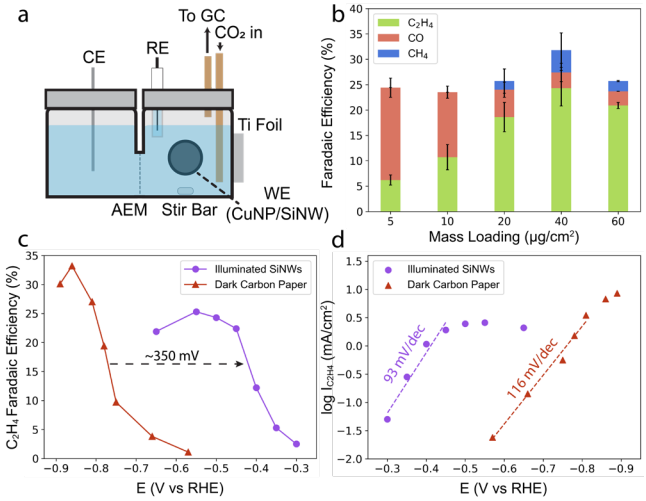

Figure 2. Photoelectrochemical performance of the CuNP/SiNW photocathode. (a) A diagram of the custom cell. The catholyte and anolyte are separated by an anion exchange membrane (AEM). (b) Mass loading dependence on the selectivity at -0.50 V vs RHE. Total products are shown in Table S2. Error bars are from 3 independent measurements. (c) Comparison of FE and (d) semi-log plots of j_{C2H4} between 40 μg/cm² CuNP on illuminated SiNWs and 69 μg/cm² CuNP on carbon paper.

The Tafel slope of the CuNP/SiNW system for CO_2R to C_2H_4 is 93 ± 14 mV/dec (Figure 2d) which is in a similar range with literature.[32] This suggests the one-electron transfer carbon-carbon coupling step as the rate-limiting step.[33] The activity of the CuNPs translate well onto SiNWs based on the semi-log of j_{C2H4} and FE_{C2H4} plots at lower potentials. However, the PEC behavior of the CuNP/SiNW quickly deviates from ideal behavior even at currents below where CO_2 mass transport limitations are expected. The maximum photocurrent is nearly reached by -0.45 V vs RHE which may explain why j_{C2H4} also plateaus. Despite increasing applied biases beyond -0.55 V vs RHE, the overall product distribution changes minimally (Table S3) compared to using carbon paper where the maximum FE_{C2H4} can reach up to 35% as more negative potentials and currents are reached.

A possible strategy for furthering a higher production rate towards C_2H_4 is to increase the mass loading of copper. An increased mass or surface area of copper has been seen to shift the selectivity towards the formation of multi-carbons.[23,34] However, when increasing mass loading beyond 40 μg/cm², there is little improvement compared to increasing from 5 μg/cm² to 40 μg/cm² (Figure 2b). As shown in Figure 1d, a monolayer coverage was almost achieved by 20 μg/cm² while additional mass loadings resulted in nanoparticles depositing

on the floor of the array (Figure S1) which may not allow those catalysts to be effectively used.

Another factor to consider is the mobility and adhesion of the CuNPs under bias. SEM images after electrolysis show structural evolution of the particles (Figure 3a) which is expected based on the behavior of these nanoparticles when they are electrochemically scrambled.[25,32] The shape of the aggregated particles and the three-dimensional nature of the substrate make it hard to quantify the density of these aggregates, but the surface qualitatively appears indistinguishable between 20, 40, and 60 μg/cm^2 (Figure S6). Given that copper has poor adhesion to silicon,[35] only 1-2 monolayers of CuNPs may adhere to the surface under bias which would explain why the density on the surface looks similar beyond 20 μg/cm^2. While this limits how many CuNPs can be effectively utilized, this keeps our system at the optimal loading density and, with the structural evolution, prevents parasitic light absorption. A tactic to increase total mass loading under bias could then be to increase the surface area of the SiNW array itself such as increasing the wire density.

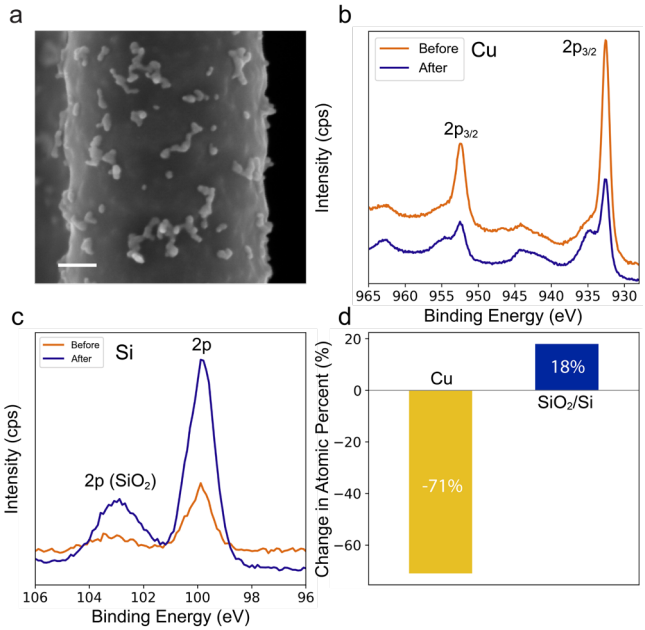

Figure 3. SEM and XPS of photocathodes after electrolysis. (a) SEM image after 1 hour electrolysis (scale bar 100 nm). XPS scans of before and after electrolysis of the (b) Cu 2p and (c) Si 2p peaks and (d) corresponding changes in atomic percent (calculations in Table S4).

X-ray photoelectron spectroscopy (XPS) of the copper and silicon peaks (Figure 3b,c, Figure S7) also reveals the changes at the surface. The measured atomic percent of copper relative to silicon decreases significantly showing that a substantial area of the silicon becomes exposed (Figure 3d) as confirmed by SEM. The Si-O peak relative to Si increases significantly after 1 hour electrolysis (Figure 3d, Table S4) which has been reported to show degradation of the photocatalytic performance.[36]

Given the target goal of operation for these systems is on the order of years,[30] it is important that the structural evolution of the CuNPs and the increased presence of SiO_2 after one hour does not lead to the rapid decay of its catalytic performance. To test the stability of the CuNP/SiNW system, the photocathode was held at -0.50 V vs RHE for over 50 hours under continuous bias and illumination (Figure 4). There was minimal change in photocurrent density with changes in selectivity observed over time. FE_{CO} remained consistent while FE_{C2H4} maintained 25% for 30 hours before decaying and FE_{CH4} steadily increased to over 10%. Even after 50 hours, j_{C2H4} remained over >1 mA/cm^2 which is the first demonstration of such stability whereas other systems show dominant HER after 1 hour.[29]

This stability can be attributed to the synergy between the n$^+$p-NWs for preventing photocorrosion and the stability of the CuNPs for CO_2R. Whereas cocatalysts used for PEC CO_2R typically employ photoelectrodeposition in which size and shape are difficult to control and could suffer from catalytic deactivation, we take advantage of colloidally synthesized nanoparticles which have already shown stability towards CO_2R.

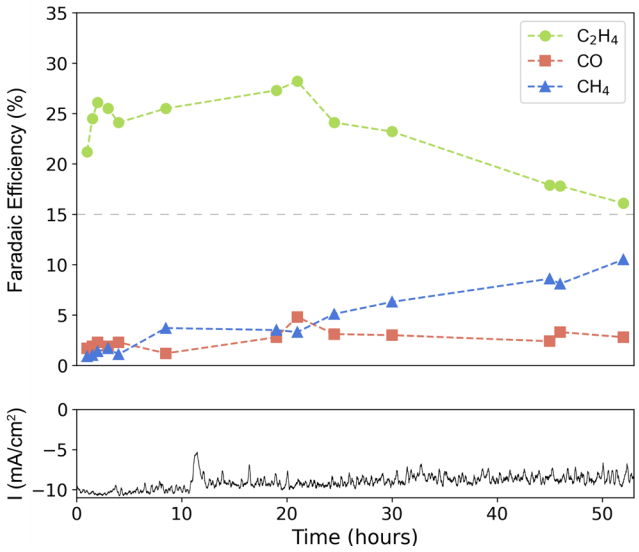

Figure 4. Stability test of the CuNP/SiNW photocathode. CuNP/SiNW was biased at -0.50 V vs RHE at 1 sun using 40 μg/cm2. The fluctuation in current density can be attributed to bubbles on the surface.

Possible reasons for the observed selectivity shift may be possible contamination of the cathode from the anode, or structural degradation of the catalyst. It's been reported that using a platinum anode results in dissolution that deposits on the cathode and shifts the selectivity away from CO_2R towards HER.[29,37] However, FE_{HER} remains steady at 60% across 50 hours and platinum is not detected through XPS (Figure S8), so platinum contamination is likely not the reason. Another possibility is that structural degradation of the copper shifts the selectivity over time,[38] but more investigation is required.

In this study, we have demonstrated how the SiNW platform can selectively drive stable PEC CO_2R towards C_2H_4. The light absorption properties of SiNWs along with its large surface area makes it an attractive platform for housing catalysts as a photocathode. Coupling this with highly active stable copper catalysts that have been extensively studied enables stable high FE_{C2H4} even on SiNWs at lower biases than its electrochemical counterpart. The structural transformation of CuNPs under bias also allows for a tolerance in mass loading without sacrificing light absorption of the underlying semiconductor. Thus, the SiNW array combined with active catalysts continues to be a model platform for furthering artificial photosynthesis to drive CO_2R towards high value products.

ASSOCIATED CONTENT

Supporting Information

The Supporting Information is available free of charge on the ACS Publications website.

Methods, additional experimental data including SEM images, XPS spectra, and electrochemical data (PDF)

AUTHOR INFORMATION

Corresponding Author

Peidong Yang – Department of Chemistry, University of California, Berkeley, California 94720, United States; Department of Materials Science and Engineering, University of California, Berkeley, California 94720, United States; Chemical Sciences Division, Lawrence Berkeley National Laboratory, Berkeley, California 94720, United States; Liquid Sunlight Alliance, Lawrence Berkeley National Laboratory, Berkeley, California 94720, United States; Kavli Energy NanoScience Institute, Berkeley, California 94720, United States; Email: p_yang@berkeley.com

Authors

Inwhan Roh – Department of Chemistry, University of California, Berkeley, California 94720, United States; Liquid Sunlight Alliance, Lawrence Berkeley National Laboratory, Berkeley, California 94720, United States

Sunmoon Yu – Department of Materials Science and Engineering, University of California, Berkeley, California 94720, United States; Chemical Sciences Division, Lawrence Berkeley National Laboratory, Berkeley, California 94720, United States

Chung-Kuan Lin – Department of Chemistry, University of California, Berkeley, California 94720, United States

Sheena Louisia – Department of Chemistry, University of California, Berkeley, California 94720, United States; Chemical Sciences Division, Lawrence Berkeley National Laboratory, Berkeley, California 94720, United States

Stefano Cestellos-Blanco – Department of Materials Science and Engineering, University of California, Berkeley, California 94720, United States

Notes

The authors declare no competing financial interests.

ACKNOWLEDGMENT

This work was supported Liquid Sunlight Alliance, which is supported by the US Department of Energy, Office of Science, Office of Basic Energy Sciences, Fuels from Sunlight Hub under award DE-SC0021266. We thank the nanofabrication facilities and entire staff in Marvell Nanofabrication Laboratory. We thank Drs. Hasan Celik, Alicia Lund, and UC Berkeley's NMR facility in the College of Chemistry (CoC-NMR) for spectroscopic assistance. Instruments in the CoC-NMR are supported in part by NIH S10OD024998. Work at the Molecular Foundry was supported by the Offices of Science, Office of Basic Energy Sciences, of the U.S. Department of Energy under Contract No. DE-AC02-05CH11231. ICP-OES was supported by the Microanalytical Facility, College of Chemistry, University of California, Berkeley. Analytical GC-MS was supported by Quantitative Biosciences at University of California, Berkeley and thank Zhongrui Zhou for the assistance.

REFERENCES

(1) De Luna, P.; Hahn, C.; Higgins, D.; Jaffer, S. A.; Jaramillio T. F.; Sargent, E. H. What would it take for renewably powered electrosynthesis to displace petrochemical processes? *Science* **2019**, 364 (6438), eeav3506. DOI: 10.1126/science.aav3506

(2) Chu, S.; Majumdar, A. Opportunities and challenges for a sustainable energy future. *Nature* **2012**, 488, 294-303. DOI: 10.1038/nature11475

(3) Turner, J. A. Sustainable Hydrogen Production. *Science* **2004**, 305 (5686), 972-974. DOI: 10.1126/science.1103197

(4) Liu, C.; Gallagher, J. J.; Sakimoto, K. K.; Nichols, E. M.; Chang, C. J.; Chang, M. C. Y.; Yang, P. Nanowire-Bacteria Hybrids for Unassisted Solar Carbon Dioxide Fixation to Value-Added Chemicals. *Nano Lett.* **2015**, 15 (5), 3634-3639. DOI: 10.1021/acs.nanolett.5b01254

(5) Liu, C.; Dasgupta, N.P.; Yang, P. Semiconductor Nanowires for Artificial Photosynthesis. *Chem. Mater.* **2014**, 26 (1), 415-422. DOI: 10.1021/cm4023198

(6) Kim, D.; Sakimoto, K. K.; Hong, D.; Yang, P. Artificial Photosynthesis for Sustainable Fuel and Chemical Production. *Angew. Chem. Int. Ed.* **2015**, 54, 3259-3266. DOI: 10.1002/anie.201409116

(7) Yang, P. Liquid Sunlight: The Evolution of Photosynthetic Biohybrids. *Nano Lett.***2021**, 21 (13), 5453-5456. DOI: 10.1021/acs.nanolett.1c02172

(8) Bard, A. J.; Fox, M. A. Artificial Photosynthesis: Solar Splitting of Water to Hydrogen and Oxygen. *Acc. Chem. Res.* **1995**, 28 (3), 141-145. DOI: 10.1021/ar00051a007

(9) Hu, Y.; Chen, F.; Ding, P.; Yang, H.; Chen, J.; Zha, C.; Li, Y. Designing effective Si/Ag interface *via* controlled chemical etching for photoelectrochemical CO_2 reduction. *J. Mater. Chem. A* **2018**, 6, 21906-21912. DOI: 10.1039/c8ta05420g

(10) Kang, U.; Lee, S.; Ham, D.; Ji, S.; Park, H. Sn-coupled p-Si Nanowire Arrays for Solar Formate Production from CO_2. *Adv. Energy Mater.* **2014**, 4, 1301614. DOI: 10.1002/aenm.201301614

(11) Zhou, B.; Ou, P.; Pant, N.; Cheng, S.; Vanka, S.; Chu, S.; Rashid, R. T.; Botton, G.; Song, J.; Mi, Z. Highly efficient binary copper-iron catalyst for photoelectrochemical carbon dioxide reduction toward methane. *Proc. Natl. Acad. Sci. U. S. A.* **2020**, 117 (3), 1330-1338. DOI: 10.1073/pnas.1911159117

(12) Li, F.; Thevenon, A.; Rosas-Hernández, A.; Wang, Z.; Li, Y.; Gabardo, C. M.; Ozden, A.; Dinh, C.; Li, J.; Wang, Y.; Edwards, J. P.; Xu, Y.; McCallum, C.; Tao, L.; Liang, Z.; Luo, M.; Wang, X.; Li, H.; O'Brien, C. P.; Tan, C.; Nam, D.; Quintero-Bermudez, R.; Zhuang, T.; Li, Y. C.; Han, Z.; Britt, R. D.; Sinton, D.; Agapie, T.; Peters, J. C.; Sargent, E. H. Molecular tuning of CO_2-to-ethylene conversion. *Nature* **2020**, 577, 509-513. DOI: 10.1038/s41586-019-1782-2

(13) Chen, Y.; Sun, K.; Audesirk, H.; Xiang, C.; Lewis, N. S. A quantitative analysis of the efficiency of solar-driven water-splitting device designs based on tandem photoabsorbers patterned with islands of metallic electrocatalysts. *Energy Environ. Sci.* **2015**, 8, 1736-1747. DOI: 10.1039/C5EE00311C

(14) Su, Y.; Liu, C.; Brittman, S.; Tang, J.; Fu, A.; Kornienko, N.; Kong, Q.; Yang, P. Single-nanowire photoelectrochemistry. *Nat. Nanotechnol.* **2016,** 11, 609-612. DOI: 10.1038/nnano.2016.30

(15) Wu, Y.; Yan, H.; Yang, P. Semiconductor nanowire array: potential substrates for photocatalysis and photovoltaics. *Top. Catal.* **2002**, 19, 197-202. DOI: 10.1023/A:1015260008046

(16) Deng, J.; Su, Y.; Liu, D.; Yang, P.; Liu, C. Nanowire Photoelectrochemistry. *Chem. Rev.* **2019**, 119 (15), 9221-9259. DOI: 10.1021/acs.chemrev.9b00232

(17) Walter, M. G.; Warren, E. L.; McKone, J. R.; Boettcher, S. W.; Mi, Q.; Santori, E. A.; Lewis, N. S. Solar Water Splitting Cells. *Chem. Rev.* **2010**, 110 (11), 6446-6473. DOI: 10.1021/cr1002326

(18) Boettcher, S. W.; Warren, E. L.; Putnam, M. C.; Santori, E. A.; Turner-Evans, D.; Kelzenberg, M. D.; Walter, M. G.; McKone, J. R.; Brunschwig, B. S.; Atwater, H. A.; Lewis, N. S. Photoelectrochemical Hydrogen Evolution Using Si Microwire Arrays. *J. Am. Chem. Soc.* **2011**, 133 (5), 1216-1219. DOI: 10.1021/ja108801m

(19) Christesen, J. D.; Zhang, X.; Pinion, C.W.; Celano, T.A.; Flynn, C. J.; Cahoon, J. F. Design Principles for Photovoltaic Devices Based on Si Nanowires with Axial or Radial p-n Junctions. *Nano Lett.* **2012**, 12 (11), 6024-6029. DOI: 10.1021/nl303610m

(20) Liu, C.; Tang, J.; Chen, H.; Liu, B.; Yang, P. A Fully Integrated Nanosystem of Semiconductor Nanowires for Direct Solar Water Splitting. *Nano Lett.* **2013**, 13 (6), 2989-2992. DOI: 10.1021/nl401615t

(21) Su, Y.; Cestellos-Blanco, S.; Min, J.; Shen, Y.; Kong, Q.; Lu, D.; Liu, C.; Zhang, H.; Cao, Y.; Yang, P. Close-Packed Nanowire-Bacteria Hybrids for Efficient Solar-Driven CO_2 Fixation. *Joule* **2020**, 4 (4), 800-811. DOI: 10.1016/j.joule.2020.03.001

(22) Kong, Q.; Kim, D.; Liu, C.; Yu, Y.; Su, Y.; Li, Y.; Yang, P. Directed Assembly of Nanoparticle Catalysts on Nanowire Photoelectrodes for Photoelectrochemical CO_2 Reduction. *Nano Lett.* **2016**, 16 (9), 5675-5680. DOI: 10.1021/acs.nanolett.6b02321

(23) Ren, D.; Fong, J.; Yeo, B.; The effects of currents and potentials on the selectivities of copper towards carbon dioxide electroreduction. *Nat. Commun.* **2018**, 9, 925. DOI: 10.1038/s41467-018-03286-w

(24) Hori, Y.; Wakebe, H.; Tsukamoto, T.; Koga, O. Electrocatalytic process of CO selectivity in electrochemical reduction of CO_2 at metal electrodes in aqueous media. *Electrochim. Acta* **1994**, 39 (11-12), 1833-1839. DOI: 10.1016/0013-4686(94)85172-7

(25) Li, Y.; Kim, D.; Louisia, S.; Xie, C.; Kong, Q.; Yu, S.; Lin T.; Aloni, S.; Fakra S. C.; Yang, P. Electrochemically scrambled nanocrystals are catalytically active for CO_2-to-multicarbons. *Proc. Natl. Acad. Sci. U. S. A.* **2020**, 117 (17), 9194-9201. DOI: 10.1073/pnas.1918602117

(26) Louisia, S.; Kim, D.; Li, Y.; Gao, M.; Yu, S.; Roh, I.; Yang, P. The presence and role of the intermediary CO reservoir in heterogeneous electroreduction of CO_2. *Proc. Natl. Acad. Sci. U. S. A.* **2022**, *In Press*. DOI: 10.1073/pnas.2201922119

(27) Reiko, H.; Tomohiro, M.; Shinji, Y.; Yoshihiro, N. Efficient Photoelectrochemical Reduction of Carbon Dioxide on a p-Type Silicon (p-Si) Electrode Modified with Very Small Copper Particles. *Chem. Lett.* **1994**, 23 (9), 1725-1728. DOI: 10.1246/cl.1994.1725

(28) Hinogami, R.; Nakamura, Y.; Yae, S.; Nakato, Y. An Approach to Ideal Semiconductor Electrodes for Efficient Photoelectrochemical Reduction of Carbon Dioxide by Modification with Small Metal Particles. *J. Phys. Chem. B* **1998**, 102 (6), 974-980. DOI: 10.1021/jp972663h

(29) Kempler, P. A.; Richter, M. H.; Cheng, W.; Brunschwig, B. S.; Lewis, N. S. Si Microwire-Array Photocathodes Decorated with Cu Allow CO_2 Reduction with Minimal Parasitic Absorption of Sunlight. *ACS Energy Lett.* **2020**, 5 (8), 2528-2534. DOI: 10.1021/acsenergylett.0c01334

(30) Pinaud, B. A.; Benck, J. D.; Seitz, L. C.; Forman, A. J.; Chen, Z.; Deutsch, T. G.; James, B. D.; Baum, K. N.; Ardo, S.; Wang, H.; Miller, E.; Jaramillo, T. F. Technical and economic feasibility of centralized facilities for solar hydrogen production *via* photocatalysis and photoelectrochemistry. *Energy Environ. Sci.* **2013**, 6 (7), 1983-2002. DOI: 10.1039/C3EE40831K

(31) Ross, M. B.; De Luna, P.; Li, Y.; Dinh, C.; Kim, D.; Yang, P.; Sargent, E. H. Designing materials for electrochemical carbon dioxide recycling. *Nat. Catal.* **2019**, 2, 648-658. DOI: 10.1038/s41929-019-0306-7

(32) Kim, D.; Kley, C. S.; Li, Y.; Yang, P. Copper nanoparticle ensembles for selective electroreduction of CO_2 to C_2-C_3 products. *Proc. Natl. Acad. Sci. U. S. A.* **2017**, 114 (40), 10560-10565. DOI: 10.1073/pnas.1711493114

(33) Liu, X.; Schlexer, P.; Xiao, J.; Ji, Y.; Wang, L.; Sandberg, R. B.; Tang, M.; Brown, K. S.; Peng, H.; Ringe, S.; Hahn, C.; Jaramillo, T. F.; Nørskov, J. K.; Chan, K. pH effects on the electrochemical reduction of $CO_{(2)}$ towards C_2 products on stepped copper. *Nat. Commun.* **2019**, 10, 32. DOI: 10.1038/s41467-018-07970-9

(34) Nitopi, S.; Bertheussen, E.; Scott, S. B.; Liu, X.; Engstfeld, A. K.; Horch, S.; Seger, B.; Stephens, I. E. L.; Chan, K.; Hahn, C.; Nørskov, J. K.; Jaramillo, T. F.; Chorkendorff, I. Progress and Perspectives of Electrochemical CO_2 Reduction on Copper in Aqueous Electrolyte. *Chem. Rev.* **2019**, 119 (12), 7610-7672. DOI: 10.1021/acs.chemrev.8b00705

(35) Oskam, G.; Long, J. G.; Natarajan, A.; Pearson, P. C. Electrochemical deposition of metals onto silicon. *J. Phys. D: Appl. Phys.* **1998**, 31, 1927-1949. DOI: 10.1088/0022-3727/31/16/001

(36) Seger, B.; Pedersen, T.; Laursen, A. B.; Vesborg, P. C. K.; Hansen, O.; Chorkendorff, I. Using TiO_2 as a Conductive Protective Layer for Photocathodic H_2 Evolution. *J. Am. Chem. Soc.* **2013**, 135 (3), 1057-1064. DOI: 10.1021/ja309523t

(37) Gurudayal; Beeman, J. W.; Bullock, J.; Wang, H.; Eichhorn, J.; Towle, C.; Javey, A.; Toma, F. M.; Matthews, N.; Ager, J. W. Si photocathode with Ag-supported dendritic Cu catalyst for CO_2 reduction. *Energy Environ. Sci.* **2019**, 12 (3), 1068-1077. DOI: 10.1039/C8EE03547D

(38) Li, Y.; Cui, F.; Ross, M. B.; Kim, D.; Sun, Y.; Yang, P. Structure-Sensitive CO_2 Electroreduction to Hydrocarbons on Ultrathin 5-fold Twinned Copper Nanowires. *Nano Lett.* **2017**, 17 (2), 1312-1317. DOI: 10.1021/acs.nanolett.6b05287

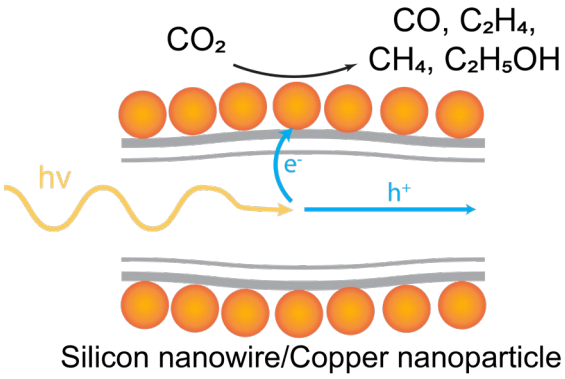
CO2
CO, C2H4,
CH4, C2H5OH
hv
e-
h+
Silicon nanowire/Copper nanoparticle

"TOC" Graphic